IEEE Access
Multidisciplinary ⋮ Rapid Review ⋮ Open Access Journal

Received 1 April 2023, accepted 11 May 2023, date of publication 22 May 2023, date of current version 26 May 2023.

Digital Object Identifier 10.1109/ACCESS.2023.3278598

RESEARCH ARTICLE

Semi-Active Control of Horizontal Vibrations for Mine Hoisting Containers Using Fuzzy Skyhook Control Strategy

XIAOJIE DENG, JIANNAN YAO, DI LIU, AND RUI YAN
School of Mechanical Engineering, Nantong University, Nantong 226019, China

Corresponding author: Jiannan Yao (yaojiannan1988@163.com)

This work was supported in part by the National Natural Science Foundation of China under Grant 51805273, in part by the Qing Lan Project of Jiangsu Province, and in part by the Priority Academic Program Development of Jiangsu Higher Education Institutions (PAPD).

ABSTRACT Mine hoisting systems have been widely used in coal mine industries. Due to a series of uncertain faults in the steel guide, serious vibrations will be excited during the operation of the machine, which will seriously influence the stability and safety of the system. In this paper, a semi-active vibration control strategy based on magnetorheological dampers was innovatively proposed. Firstly, a reasonable simplified dynamic model of mine hoisting system was established. Secondly, the simulation results from the virtual prototype model were used to verify the rationality of the established dynamic model. Then, a fuzzy skyhook damping semi-active control scheme based on magnetorheological dampers was designed. Finally, the availability of this vibration control scheme was verified by the Adams/Simulink co-simulation technique. The root mean square (RMS), mean and maximum values of the horizontal vibration acceleration of the container were reduced by 47.32%, 22.50% and 35.39%, respectively. The fuzzy skyhook damping semi-active control strategy of good stability can well suppress the horizontal vibrations of the mine hoisting system.

INDEX TERMS Semi-active control, fuzzy skyhook damping control, magnetorheological dampers, mine hoisting systems.

I. INTRODUCTION

The mine hoist is a key equipment in mine transportations. As the increase of the hoisting velocity and load of the mine hoisting systems, higher requirements are being required on guiding devices in order to ensure the stability and safety of the machine [1]. In the hoisting processes when the machine is operating at a high speed, rigid guides are used to guide and suppress the horizontal vibrations of the hoisting containers [2]. However, severe working conditions and installation errors of rigid guides will intensify the vibration of the mine hoisting system. Some studies have shown that rigid guide misalignment failures have a more serious impact on the vibration of mine hoisting systems than other failures [3]. When the roller cage shoe passes the step for a short time, a strong impact will be induced between the guide shoe and hoisting conveyance, which will seriously affect the safety of the system. Thus, it is essential to study the impact effects of the rigid guides of mine hoisting systems, and a certain control strategy is also required to suppress the horizontal vibrations of the conveyance.

There have been many studies on the research of vibration mechanism of mine hoisting systems. Kaczmarczyk et al. [4] have derived a distributed-parameter mathematical model of deep mine hoisting cables using the classical moving co-ordinate frame approach and Hamilton's principle. They have investigated the dynamic behaviour of deep mine hoisting cables, and the results showed that the response of the catenary-vertical rope system may have many resonance phenomena, including external, parametric and autoparametric resonances. Wang et al. [5] have studied the effect of terminal mass on fretting and fatigue parameters of the hoisting

The associate editor coordinating the review of this manuscript and approving it for publication was Xiaojie Su.

rope. When the terminal mass increases from 1000 kg to 1700 kg, there is a significant increase in the fretting and fatigue parameters of the wire rope, which will shorten the service life of the rope. Wang et al. [6] have derived the equations of motion of the multi-cable suspension platform using the Lagrange equation with constraints, and Adams software was used to verify the correctness of the model. The simulation results of the equations of motion showed that the model is able to better represent the dynamics of the multi-cable suspension platform. Wang et al. [7] have modelled the longitudinal vibration of a parallel hoisting system with time-varying wire ropes, and the validity of the model has been verified by ADAMS simulation results. They have carried out numerical simulations with different excitations and the results of the study have shown that the system acceleration significantly increases the longitudinal vibration of the wire rope. Guo et al. [8] have studied the dynamic responses of wire ropes in friction hoisting systems subjected to different periodic excitations. Transverse, longitudinal, and coupled vibrations have been analysed by time-frequency analysis. The results showed that the transverse vibration is a forced vibration following the excitation, while the longitudinal vibration is a complex, random state. Wu et al. [9] have developed a coupling longitudinal-transverse model of the mine friction hoist using the Hamilton's principle and discretized the partial differential equations using the modified Galerkin's method. The relationship between the load, velocity and transverse vibration of rope has been analysed by means of this model. Cao et al. [10] have studied a rope-guided hoisting system with the tension difference between two guiding ropes and found out that the appropriate tension difference and distance difference is beneficial in reducing the maximum lateral displacement of the hoisting container. Yang et al. [11] have derived a dynamical model for the coupled vibrations of building and elevator ropes based on the Hamilton's principle, and an experimental testbed was built to validate the mathematical model. The proposed theoretical model can be effectively used to predict the vibrations of real building and elevator ropes.

Based on the vibration mechanism of mine hoisting systems, there have been many researchs in the vibration control of mine hoisting systems. Wang et al. [12] have applied the backstepping method and active disturbance rejection control (ADRC) to design a controller under the floating sheave to suppress longitudinal vibrations of the hoisting system by considering the influence of external disturbances and elasticity of the wire rope. Li et al. [13] have proposed an adaptive fuzzy sliding mode controller using Liapunov theory which takes into account the effects of external disturbances and parameter uncertainties, and a wire rope tension coordination control system was designed. Yao et al. [14] have innovatively proposed a wire rope tension equilibrator with magnetorheological dampers, and proved that the new wire rope tension equilibrator is effective in suppressing shock vibrations in mine hoisting systems. Li et al. [15] have designed a stiffness experimental platform in order to analyze the stiffness of the roller cage shoe, and the safety and smoothness of mine hoisting container were improved by adjusting the stiffness of roller cage shoes. Chen et al. [16] have developed a mathematical model of the elevator system driven by a permanent magnet synchronous motor, and the dynamic response characteristics and energy dissipation characteristics of the elevator system were analyzed. A sliding mode controller has been designed to control the system and the robustness and tracking control performance of the controller have been verified through numerical simulation. Although there has been some significant work about the vibration control in mine hoisting systems, few scholars have mentioned the design of vibration controllers and actuators in the roller cage shoe. The existing actuators for vibration control are mainly floating sheaves [17], which mainly suppress vibration from the source of disturbance. There are limitations to the control effect due to many unknown disturbances in the wire rope from the floating sheave to the mine hoisting container [18], e.g. turbulent disturbances in the shaft [19]. At the same time, due to the length of the wire rope, there is a time lag in the transmission of the control action from the floating sheave to the mine hoisting container [20]. The wire rope tension coordination controller mainly controls the dynamic load and uneven tension of the wire rope, thus improving the smoothness and safety of the mine hoisting system [21]. As the mine hoisting vessel rises and falls, the length and mass of the hoisting wire rope constantly change, and this time-varying characteristic makes the system severely nonlinear [22]. There are few control strategies to directly control the horizontal vibrations of mine hoisting container.

In this paper, a semi-active controller to reduce the horizontal vibrations of the mine hoisting container was designed based on magnetorheological dampers. The semi-active control solution based on magnetorheological dampers uses lighter actuators than the hydraulic cylinders, and the semi-active control solution suppresses vibrations without deteriorating the stability of the system. This paper proposed a new approach for vibration control in mine hoisting systems.

II. DERIVATION AND VALIDATION OF THE DYNAMIC MODEL FOR MINE HOISTING SYSTEM

A. DYNAMIC MODEL FOR MINE HOISTING SYSTEM

The winding mine hoisting system mainly consists of rigid guides, roller cage shoes, wire rope and hoisting container, and its structural sketch was shown in Fig.1. The interaction between the roller cage shoe and the rigid guide in the *XOZ* plane is the main source of horizontal vibration of the mine hoisting container. This paper focuses on the effect of the interaction between the roller cage shoe and the rigid guide on the horizontal vibration of the hoist, without considering the coupling effect of the wire rope vibration and the horizontal vibration of the mine hoisting container. Therefore, in order to reasonably reduce the complexity of the model and suppress the horizontal vibration of the mine hoisting vessel more

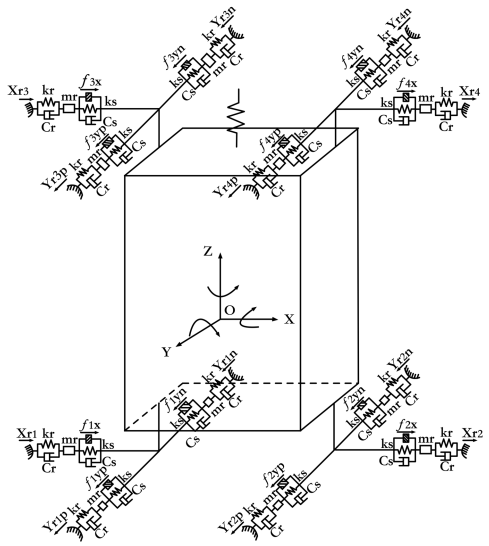

FIGURE 1. Sketch of mine hoisting conveyance.

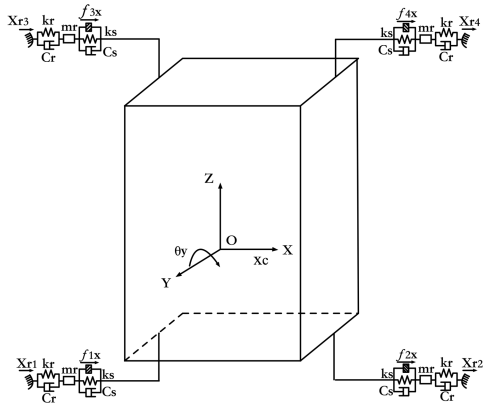

FIGURE 2. Simplified model of mine hoisting conveyance.

efficiently, the dynamic model for the winding mine hoisting system in this study was shown in Fig.2.

According to Newton's second law, the centre-of-mass displacement x_c of the container and the angle of rotation θ_y of the container satisfy the relationship:

$$mx_c = F_{x1} + F_{x3} - F_{x2} - F_{x4} \tag{1}$$
$$J\ddot{\theta}_y = (F_{x2} - F_{x1})\, l_{h1} + (F_{x3} - F_{x4})\, l_{h2} \tag{2}$$

where m is the mass of the hoisting container, J is the rotational inertia of the hoisting container around the OY axis, l_{h1} is the distance between the lower roller cage shoe and the centre of mass of the container, and l_{h2} is the distance between the upper roller cage shoe and the centre of mass of the container.

The expressions for F_{x1}, F_{x2}, F_{x3} and F_{x4} are as follows

$$\begin{aligned} F_{x1} &= k_s\left(l_{h1}\theta_y - x_c + x_1\right) \\ &\quad + c_s\left(l_{h1}\dot{\theta}_y - \dot{x}_c + \dot{x}_1\right) + f_{1x} \\ F_{x2} &= k_s\left(-l_{h1}\theta y + x_c - x_2\right) \\ &\quad + c_s\left(-l_{h1}\dot{\theta}_y + \dot{x}_c - \dot{x}_2\right) + f_{2x} \\ F_{x3} &= k_s\left(-l_{h2}\theta_y - x_c + x_3\right) \\ &\quad + c_s\left(-l_{h2}\dot{\theta}_y - \dot{x}_c + \dot{x}_3\right) + f_{3x} \\ F_{x4} &= k_s\left(l_{h2}\theta_y + x_c - x_4\right) \\ &\quad + c_s\left(l_{h2}\dot{\theta}_y + \dot{x}_c - \dot{x}_4\right) + f_{4x} \end{aligned} \tag{3}$$

where x_1, x_2, x_3 and x_4 are the horizontal displacements of roller cage shoes 1, 2, 3 and 4, respectively; k_s is the cushioning stiffness of the roller cage shoe; c_s is the cushioning damping of the roller cage shoe; f_{1x}, f_{2x}, f_{3x} and f_{4x} are the controllable cushioning forces of roller cage shoes 1, 2, 3 and 4, respectively.

Substituting equation (3) into equations (1) and (2) as follows

$$\begin{aligned} m\ddot{x}_c &= -4k_s x_c + 2k_s\left(l_{h1} - l_{h2}\right)\theta_y \\ &\quad - 4c_s\dot{x}_c + 2c_s\left(l_{h1} - l_{h2}\right)\dot{\theta}_y \\ &\quad + k_s x_1 + k_s x_2 + k_s x_3 + k_s x_4 \\ &\quad + c_s\dot{x}_1 + c_s\dot{x}_2 + c_s\dot{x}_3 + c_s\dot{x}_4 \\ &\quad + f_{1x} - f_{2x} + f_{3x} - f_{4x} \end{aligned} \tag{4}$$

$$\begin{aligned} J\ddot{\theta}_y &= 2\,k_s\left(l_{h1} - l_{h2}\right)x_c + 2k_s\left(-l_{h1}^2 - l_{h2}^2\right)\theta_y \\ &\quad + 2c_s\left(l_{h1} - l_{h2}\right)\dot{x}_c + 2c_s\left(-l_{h1}^2 - l_{h2}^2\right)\dot{\theta}_y \\ &\quad - k_s l_{h1}x_1 - k_s l_{h1}x_2 + k_s l_{h2}x_3 + k_s l_{h2}x_4 \\ &\quad - c_s l_{h1}\dot{x}_1 - c_s l_{h1}\dot{x}_2 + c_s l_{h2}\dot{x}_3 + c_s l_{h2}\dot{x}_4 \\ &\quad - l_{h1}f_{1x} + l_{h1}f_{2x} + l_{h2}f_{3x} - l_{h2}f_{4x} \end{aligned} \tag{5}$$

The expressions for x_1, x_2, x_3 and x_4 are as follows

$$\begin{aligned} m_r\ddot{x}_1 &= k_r\left(x_{r1} - x_1\right) + c_r\left(\dot{x}_{r1} - \dot{x}_1\right) - F_{x1} \\ m_r\ddot{x}_2 &= k_r\left(x_{r2} - x_2\right) + c_r\left(\dot{x}_{r2} - \dot{x}_2\right) + F_{x2} \\ m_r\ddot{x}_3 &= k_r\left(x_{r3} - x_3\right) + c_r\left(\dot{x}_{r3} - \dot{x}_3\right) - F_{x3} \\ m_r\ddot{x}_4 &= k_r\left(x_{r4} - x_4\right) + c_r\left(\dot{x}_{r4} - \dot{x}_4\right) + F_{x4} \end{aligned} \tag{6}$$

where m_r is the mass of the roller cage shoe, k_r is the contact stiffness of the roller cage shoe, c_r is the contact damping of the roller cage shoe, x_{r1}, x_{r2}, x_{r3} and x_{r4} are the displacement excitations of the rigid guides to the roller cage shoe 1, 2, 3 and 4, respectively.

Substituting equation (3) into equation (6) yields

$$\begin{aligned} m_r\ddot{x}_1 &= k_s x_c - k_s l_{h1}\theta_y + c_s\dot{x}_c - c_s l_{h1}\dot{\theta}_y \\ &\quad - \left(k_s + k_r\right)x_1 - \left(c_s + c_r\right)\dot{x}_1 \\ &\quad + k_r x_{r1} + c_r\dot{x}_{r1} - f_{1x} \\ m_r\ddot{x}_2 &= k_s x_c - k_s l_{h1}\theta_y + c_s\dot{x}_c - c_s l_{h1}\dot{\theta}_y \\ &\quad - \left(k_s + k_r\right)x_2 - \left(c_s + c_r\right)\dot{x}_2 \\ &\quad + k_r x_{r2} + c_r\dot{x}_{r2} + f_{2x} \\ m_r\ddot{x}_3 &= k_s x_c + k_s l_{h2}\theta_y + c_s\dot{x}_c + c_s l_{h2}\dot{\theta}_y \\ &\quad - \left(k_s + k_r\right)x_3 - \left(c_s + c_r\right)\dot{x}_3 \\ &\quad + k_r x_{r3} + c_r\dot{x}_{r3} - f_{3x} \\ m_r\ddot{x}_4 &= k_s x_c + k_s l_{h2}\theta_y + c_s\dot{x}_c + c_s l_{h2}\dot{\theta}_y \\ &\quad - \left(k_s + k_r\right)x_4 - \left(c_s + c_r\right)\dot{x}_4 \\ &\quad + k_r x_{r4} + c_r\dot{x}_{r4} + f_{4x} \end{aligned} \tag{7}$$

To simulate the dynamic model in the Matlab/Simulink environment, the above equations were transformed into the form of the state space. Construct the variable **q**, **s** and **r**

$$\begin{aligned}\mathbf{q} &= [x_c \quad \theta_y]^T \\ \mathbf{s} &= [x_1 \quad x_2 \quad x_3 \quad x_4]^T \\ \mathbf{r} &= [x_{r1} \quad x_{r2} \quad x_{r3} \quad x_{r4}]^T\end{aligned} \tag{8}$$

Construct state variable **X**, **U** and **W**

$$\mathbf{X} = \begin{bmatrix}\mathbf{q}\\ \mathbf{s}\\ \dot{\mathbf{q}}\\ \dot{\mathbf{s}}\end{bmatrix} \quad \mathbf{U} = \begin{bmatrix}f_{1x}\\ f_{2x}\\ f_{3x}\\ f_{4x}\end{bmatrix} \quad \mathbf{W} = \begin{bmatrix}\mathbf{r}\\ \dot{\mathbf{r}}\end{bmatrix} \tag{9}$$

Combining equations (4), (5), (7), and (9), the state space equation for the mine hoisting system was expressed as

$$\dot{\mathbf{X}} = \mathbf{AX} + \mathbf{BU} + \mathbf{RW} \tag{10}$$

where the matrix **AX**, **BU** and **RW** are

$$\mathbf{AX} = \begin{bmatrix}\mathbf{O}_{2\times2} & \mathbf{O}_{2\times4} & \mathbf{I}_{2\times2} & \mathbf{O}_{2\times4}\\ \mathbf{O}_{4\times2} & \mathbf{O}_{4\times4} & \mathbf{O}_{4\times2} & \mathbf{I}_{4\times4}\\ \mathbf{M}_c^{-1}\mathbf{K}_1 & \mathbf{M}_c^{-1}\mathbf{K}_2 & \mathbf{M}_c^{-1}\mathbf{C}_1 & \mathbf{M}_c^{-1}\mathbf{C}_2\\ \mathbf{M}_r^{-1}\mathbf{K}_3 & \mathbf{M}_r^{-1}\mathbf{K}_4 & \mathbf{M}_r^{-1}\mathbf{C}_3 & \mathbf{M}_r^{-1}\mathbf{C}_4\end{bmatrix}\begin{bmatrix}\mathbf{q}\\ \mathbf{s}\\ \dot{\mathbf{q}}\\ \dot{\mathbf{s}}\end{bmatrix}$$

$$\mathbf{BU} = \begin{bmatrix}\mathbf{O}_{2\times4}\\ \mathbf{O}_{4\times4}\\ \mathbf{M}_c^{-1}\mathbf{N}_1\\ \mathbf{M}_r^{-1}\mathbf{N}_2\end{bmatrix}\begin{bmatrix}f_{1x}\\ f_{2x}\\ f_{3x}\\ f_{4x}\end{bmatrix}$$

$$\mathbf{RW} = \begin{bmatrix}\mathbf{O}_{2\times4} & \mathbf{O}_{2\times4}\\ \mathbf{O}_{4\times4} & \mathbf{O}_{4\times4}\\ \mathbf{O}_{2\times4} & \mathbf{O}_{2\times4}\\ \mathbf{M}_r^{-1}\mathbf{K}_5 & \mathbf{M}_r^{-1}\mathbf{C}_5\end{bmatrix}\begin{bmatrix}\mathbf{r}\\ \dot{\mathbf{r}}\end{bmatrix}$$

where the intermediate transition matrices are

$$\mathbf{M}_c = \begin{bmatrix}m & \\ & J\end{bmatrix} \quad \mathbf{M}_r = \begin{bmatrix}m_r & & & \\ & m_r & & \\ & & m_r & \\ & & & m_r\end{bmatrix}$$

$$\mathbf{N}_1 = \begin{bmatrix}1 & -1 & 1 & -1\\ -l_{h1} & l_{h1} & l_{h2} & -l_{h2}\end{bmatrix}$$

$$\mathbf{N}_2 = \begin{bmatrix}-1 & & & \\ & 1 & & \\ & & -1 & \\ & & & 1\end{bmatrix}$$

$$\mathbf{K}_1 = \begin{bmatrix}-4k_s & 2\,k_s\,(l_{h1}-l_{h2})\\ 2\,k_s\,(l_{h1}-l_{h2}) & 2\,k_s\,(-l_{h1}^2-l_{h2}^2)\end{bmatrix}$$

$$\mathbf{C}_1 = \begin{bmatrix}-4c_s & 2\,c_s\,(l_{h1}-l_{h2})\\ 2\,c_s\,(l_{h1}-l_{h2}) & 2\,c_s\,(-l_{h1}^2-l_{h2}^2)\end{bmatrix}$$

$$\mathbf{K}_2 = \begin{bmatrix}K_s & K_s & K_s & K_s\\ -K_s l_{h1} & -K_s l_{h1} & K_s l_{h2} & K_s l_{h2}\end{bmatrix}$$

$$\mathbf{C}_2 = \begin{bmatrix}c_s & c_s & c_s & c_s\\ -c_s l_{h1} & -c_s l_{h1} & c_s l_{h2} & c_s l_{h2}\end{bmatrix}$$

$$\mathbf{K}_3 = \begin{bmatrix}k_s & -k_s l_{h1}\\ k_s & -k_s l_{h1}\\ k_s & k_s l_{h2}\\ k_s & k_s l_{h2}\end{bmatrix} \quad \mathbf{C}_3 = \begin{bmatrix}c_s & -c_s l_{h1}\\ c_s & -c_s l_{h1}\\ c_s & c_s l_{h2}\\ c_s & c_s l_{h2}\end{bmatrix}$$

$$\mathbf{K}_4 = \begin{bmatrix}-k_s-k_r & & & \\ & -k_s-k_r & & \\ & & -k_s-k_r & \\ & & & -k_s-k_r\end{bmatrix}$$

$$\mathbf{C}_4 = \begin{bmatrix}-c_s-c_r & & & \\ & -c_s-c_r & & \\ & & -c_s-c_r & \\ & & & -c_s-c_r\end{bmatrix}$$

$$\mathbf{K}_5 = \begin{bmatrix}k_r & & & \\ & k_r & & \\ & & k_r & \\ & & & k_r\end{bmatrix}$$

$$\mathbf{C}_5 = \begin{bmatrix}c_r & & & \\ & c_r & & \\ & & c_r & \\ & & & c_r\end{bmatrix}$$

B. SIMULINK SIMULATION MODEL FOR MINE HOISTING SYSTEM

The state space equation above was modelled in Matlab/Simulink for simulation. In this paper, the parameters of a mine hoisting system was used for simulation. The specific simulation parameters were shown in Table 1.

TABLE 1. Simulation parameters for mine hoisting system.

Parameters	Notation	Numerical value
Quality of hoisting container	m	34 000 kg
Rotational inertia of hoisting container	J	234 000 kg·m^2
The quality of roller cage shoe	m_r	46 kg
Cushioning stiffness of roller cage shoe	k_s	1 000 000 N/m
Cushioning damping of roller cage shoe	c_s	16 000 N·s/m
Contact stiffness of roller cage shoe	k_r	1 700 000 N/m
Distance between the lower roller cage shoe and the centre of mass of hoisting container	l_{h1}	4.5 m
Distance between the upper roller cage shoe and the centre of mass of hoisting container	l_{h2}	4.5 m
Radius of the roller cage shoe	r	0.175 m

Studies have shown that rigid guide misalignment failures have a more serious impact on the vibrations of mine hoisting systems than other rigid guide failures [1]. In this paper, the hoist was supposed to operate at a lifting speed of 9 m/s and pass over a step with a height of 2 cm. The step function was used in Simulink to simulate the step, and since both sides of the rigid guides are symmetrical, it is assumed that the step failure is located on one side only.

During the hoisting process of the mine hoisting container, there is a time lag in impact excitation between the upper and lower roller cage shoes beacuse the hoisting container has a

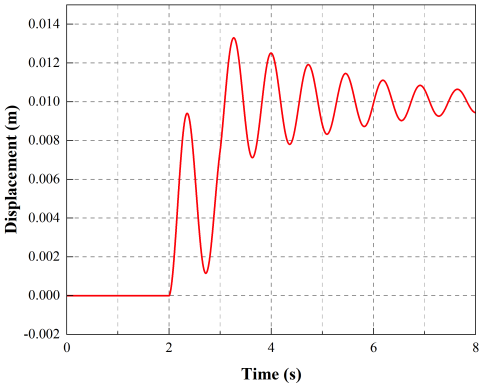

FIGURE 3. Displacement response at the centre of mass of hoisting container.

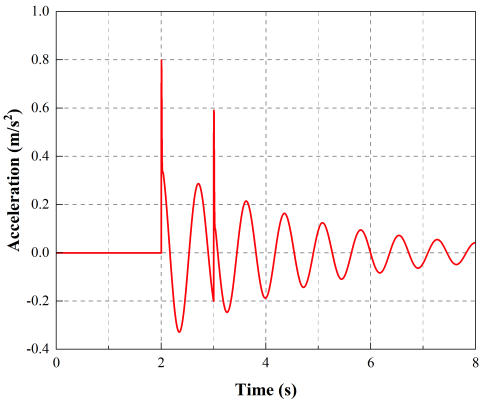

FIGURE 4. Acceleration response at the centre of mass of hoisting container.

certain height. The lag time Δt can be calculated as:

$$\Delta t = (l_{h1} + l_{h2}) / v_z$$

where v_z is the lifting speed of the hoisting container.

C. SIMULATION RESULTS

A rigid guide misalignment failure was adopted as the input for the simulink model. The vibration displacement and acceleration at the centre of mass of the hoisting container were the outputs from the simulation, and the vibration displacement and acceleration were used as the stability indicators of the hoisting container. The vibration responses of the hoisting container under the influence of the rigid guide misalignment failure were shown in Figs.3 and 4.

III. ADAMS VIRTUAL PROTOTYPE FOR MINE HOISTING SYSTEM

The mathematical model of the mine hoisting system established in this paper has been heavily simplified in the modelling, so the simulation results of the dynamic model deviate to some extent from the operation of the actual mine hoisting system. In this paper, the correctness of the dynamic model was verified using the virtual prototype technology. The virtual prototype was constructed on the Adams platform

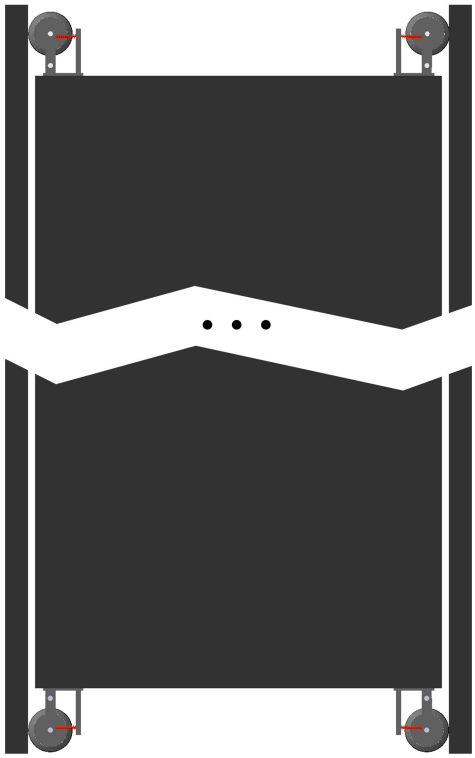

FIGURE 5. Adams model for the mine hoisting system.

with the same mine hoisting system parameters to verify the rationality of the dynamic model and the virtual prototype.

A. ADAMS VIRTUAL PROTOTYPE MODEL

As the three-dimensional(3D) modelling capability of Adams is not very strong and the built model is relatively crude, Solidworks platform was used to build the 3D model of the mine hoisting system. After the model was imported to Adams, the material, mass, constraints and contact forces of the imported model needed to be set.Therefore, some necessary model parameters and motion relationships should be manually added to the Adams model. The 3D model constructed was shown in Fig.5.

In order to verify the rationality of the dynamic numerical model, the parameters of the Adams model should be consistent with the dynamic model, and the specific values were shown in Table 1. The hoisting speed and excitation action time of the mine hoisting container should also be consistent, so the hoisting speed of the mine hoist container in the Adams model was 9 m/s. The simulation time was set to 8 s and the number of simulation steps was 8000.The horizontal displacement and acceleration of the centre of mass of the hoisting container were the simulation ouputs.

B. SIMULATION TO VALIDATE SIMULINK DYNAMIC MODEL

After the completement of the virtual prototyping simulation for the mine hoisting system, the horizontal displacement and the horizontal acceleration at the centre of mass of the

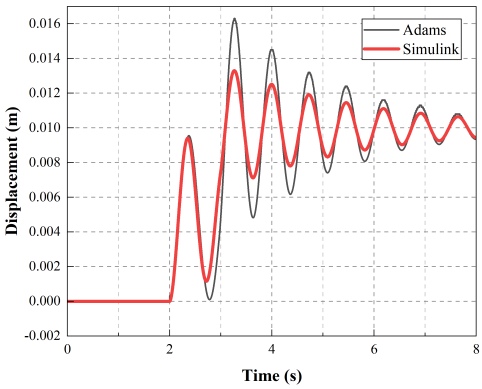

FIGURE 6. Displacement response at the centre of mass of hoisting container.

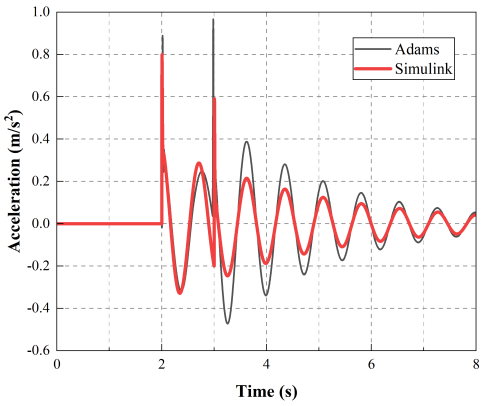

FIGURE 7. Acceleration response at the centre of mass of hoisting container.

hoisting container were measured. The simulation results from the Adams model were compared with those from the numerical model to verify the correctness of the numerical model. The simulation results were shown in Figs.6 and 7.

The results from the two models were well consistent to each other as shown in Figs.6 and 7. The vibration frequencies of the hoisting container vibration are basically the same, and the vibration amplitude from the Adams model is slightly higher than that from the numerical model. The two models obtain the same output results with the same parameters, which verifies the consistency of the two models and proves the rationality of the mine hoisting system dynamic model.

After the reasonability of the established Adams model has been verified, a parametric sensitivity analysis was also carried out. Sensitivity analysis is a good method to study the importance of one input parameter to the model outputs. In the process of the sensitivity analysis simulation, only one model parameter was continuously varied by keeping the other input parameters constant to investigate the change rule of the corresponding output. The sensitivity analysis was conducted using the corresponding parameters shown in Tables 1 and 2. The first excited impact acceleration of the container when the conveyance is passing through the fault

TABLE 2. The model parameters for the sensitivity analysis.

Parameters	Value
Quality of hoisting container	30 600 kg - 37 400 kg
Cushioning stiffness of roller cage shoe	900 000 N/m - 1 100 000 N/m
Cushioning damping of roller cage shoe	14 400 N·s/m - 17 600 N·s/m
Lifting speed	8.1 m/s - 9.9 m/s
Height of step	2.2 cm - 1.8 cm

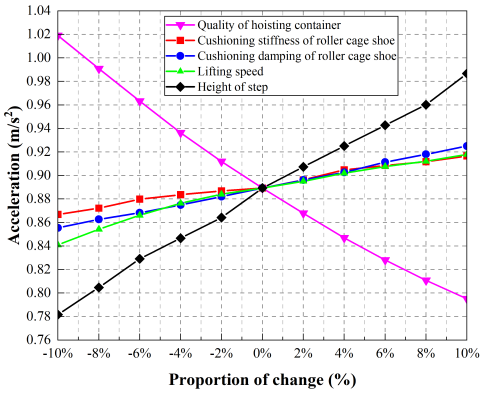

FIGURE 8. The parametric sensitivity analysis.

step was used as the evaluation index for the vibration control. And Fig.8 has demonstrated the correlations between the multiple model input parameters and the evaluation index.

The results of the sensitivity analysis showed that the higher the mass of the hoisting container, the lower the impact acceleration on the container. And the higher the value of the other parameters, the higher the impact acceleration on the container. The impact acceleration is most sensitive to the change in the mass of the container due to the large mass of the mine hoisting container. The height of the step is also a major factor in the impact acceleration. Then, the impact acceleration is less sensitive to the changes in other parameters.

IV. SIMULINK MODEL OF MAGNETORHEOLOGICAL DAMPERS

In this paper, the control scheme for the horizontal vibration suppression of hoisting container was further explored. Magnetorheological dampers have been widely used for vibration suppression in automotive suspensions, bridges, buildings, high-speed trains and lifts [23] due to their low power consumption, rapid response, high damping force and adjustability [24]. In this paper, magnetorheological damper was used as an actuator for horizontal vibration suppression of the mine hoist container. The mathematical model of a magnetorheological damper was used in Simulink instead of an actuator, and an appropriate control strategy was designed to suppress horizontal vibrations of the container.

A. MAGNETORHEOLOGICAL DAMPERS

Magnetorheological dampers are commonly used as semi-active damping devices, which have the advantages of small size, good performance and high cost performance. The output damping force of a magnetorheological damper can be adjusted by varying the coil current of the damper [25]. Magnetorheological dampers are excellent semi-active damping devices because of their ability to switch damping forces quickly and their low energy dissipation. Magnetorheological dampers are now widely used for vibration suppression in automotive suspensions, bridges, buildings, high-speed trains and lifts, and have achieved very good suppression results. Magnetorheological liquids are intelligent materials combining micron-sized magnetic particles with high magnetic permeability, non-magnetic carrier liquids and stabilisers. The magnetorheological fluid can change from a well-flowing Newtonian fluid to a Bingham body in an instant(on the order of milliseconds) when subjected to a changing magnetic field. And this change is continuous, controllable and reversible. Magnetorheological fluids are characterized by high yield strength, wide damping range, fast response and good stability. These characteristics make magnetorheological fluids a good material for intelligent dampers. The working modes of magnetorheological fluids can be classified as flow mode, shear mode, squeeze mode and mixing mode.

The dynamical performance of magnetorheological dampers is not only related to the applied magnetic field and the motion state of the piston, but also to the characteristics of the external excitation. Magnetorheological dampers have non-linear properties such as hysteresis, double viscosity and saturation [26], which may causes many problems for the accurate modelling of magnetorheological dampers. Many different models of magnetorheological dampers have been proposed based on the hysteresis, double viscosity and saturation properties of magnetorheological dampers. Common models contain the Bingham model, Bouc-Wen model, hyperbolic tangent model, polynomial model, etc., which have different accuracy and complexity. In general, the more accurate the model, the more complex it is. A magnetorheological damper dynamic model should be chosen according to the the accuracy we need.

The complexity of the magnetorheological damper model will influence the difficulty in designing the controller. In addition, the accuracy of the model will influence the control effect. Therefore, to make it easy to design the controller, the accuracy of the model of MR damper should be improved upto a good level. The Bingham model is simple in form, but it can only express the yield characteristics of magnetorheological dampers. The Bingham model cannot express the hysteretic and nonlinear characteristics of magnetorheological fluids when the magnetorheological damper is operating at low speeds. Its inverse model is relatively easy to obtain, but the accuracy of the model is limited. Bouc-Wen model can express the yield characteristics and the hysteretic characteristics of MR dampers and it has a high model accuracy. However, the Bouc-Wen model applies two differential equations to express the dynamical characteristics of MR dampers, so it is too complex. And its inverse model ignores the hysteretic effects, so the predicted control current is less accurate when the damper is operating at low speeds. In the polynomial model, two polynomial functions are used to fit the dynamic curve of the magnetorheological damper. However, the polynomial model can only well express the hysteresis effect of the damping force when the order of the polynomial model is higher than 5. A polynomial model of too high order is a complex mathematical model and its inverse model is also difficult to solve. The magnetorheological damper model based on segmentation functions is able to express the hysteretic effect of dampers to some extent. However, it does not express the yield characteristics of magnetorheological dampers well due to its unsmooth dynamic curve.

The accuracy, complexity and reversibility should be considered when choosing a reasonable MR damper model. And the hysteretic and nonlinear characteristics of the magnetorheological dampers should also be considered into the mathematical model. In the hyperbolic tangent model, linear functions are used to express the damping and stiffness properties of magnetorheological dampers. The hyperbolic tangent model contains only a simple hyperbolic tangent function, so its parameters can be easily identified. The hyperbolic tangent model is able to fit the damping force curve of magnetorheological dampers smoothly. It can well expresses the hysteretic and yield characteristics of magnetorheological dampers. The damping forces of the model do not change abruptly in the non-linear region. As the hyperbolic tangent model contains only one hyperbolic tangent function, it is possible to directly solve the inverse model expressions.

B. HYPERBOLIC TANGENT MODEL FOR MAGNETORHEOLOGICAL DAMPERS

Among many dynamical models for magnetorheological dampers, the hyperbolic tangent model can well expresses the hysteresis and yield characteristics of magnetorheological dampers. The hyperbolic tangent model for magnetorheological dampers is simple in form and relatively accurate, so it is well suited for controller design. Therefore, the hyperbolic tangent model was used as the dynamical model of the magnetorheological damper.

The mathematics of the hyperbolic tangent model was expressed as

$$f = f_y tanh(a_1\dot{x} + a_2 x) + c\dot{x} + kx + f_0 \tag{11}$$

where f_y is the yield force level of the hysteretic component, a_1 and a_2 are the arguments of the hyperbolic tangent function, f_0 is the offset of damper force, k is the stifiness coeficient of the spring, and c is the viscous coeffcient of the dashpot.

The hyperbolic tangent model of magnetorheological dampers used in this paper was cited from Wei Shuli's research results [27]. The parameters of the

TABLE 3. Identification parameters for hyperbolic tangent model of magnetorheological damper.

Parameters	I: 0-0.2A	I: 0.2A-1A
f_y	579.6I+82.96	-719.6I^2+1817I-135.7
f_0	-19.95I-11.77	16.28I^2-29.55I-11.67
c	3.1I+0.71	0.1429I^2+2.669I+0.84
k	0.27	0.27
a_1	0.100	0.075
a_2	0.065	0.080

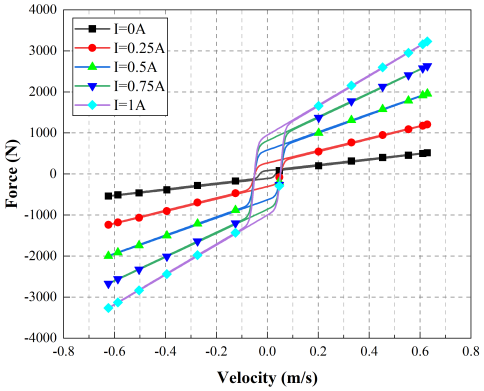

FIGURE 9. Damping force versus velocity under different electric current.

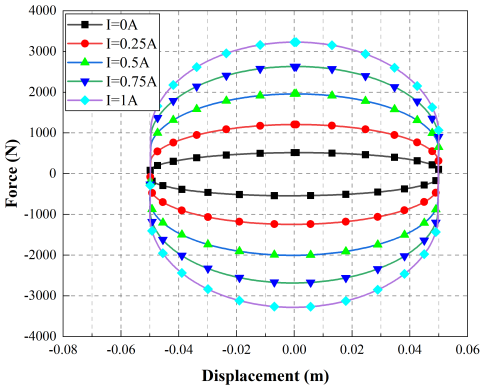

FIGURE 10. Damping force versus displacement under different electric current.

magnetorheological damper were shown in Table 3, where a_1, a_2 and k are considered to be constant values, then f_y, f_0 and c are different functions of the coil current.

The hyperbolic tangent model of the magnetorheological damper was established in Simulink. A sinusoidal excitation signal with an amplitude of 5 cm and a frequency of 2 Hz was fed into the magnetorheological damper model. The damping force, relative velocity and relative displacement of the magnetorheological damper model were output under different current conditions. The Force-Velocity and Force-Displacement diagrams of the magnetorheological damper were shown in Figs.9 and 10.

From the simulation results, it can be seen that the model can effectively express the hysteresis characteristics and double viscosity characteristics of the magnetorheological damper. When the coil current was set to the maximum value, the output damping force was the highest and the energy dissipation is best.

V. ADAMS/SIMULINK CO-SIMULATIONN OF HORIZONTAL VIBRATION SUPPRESSION

Although the mathematical model of the mine hoisting system can be used to obtain some simulation conclusions, there are more simplified operations in the mathematical model. There are some inevitable modelling errors in the mathematical model. In order to study the characteristics of the system more realistically, the simulation process of the mine hoisting system was carried out in the Adams environment. Then, the calculation process of the vibration control for the mine hoisting system was carried out in Simulink to compensate the lack of control calculation capability in the Adams platform. Finally, the Adams/Simulink co-simulation control based on the virtual prototype was established.

A. VIBRATION CONTROL STRATEGIES FOR HOISTING CONTAINERS

During the operation of the mine hoisting system, the fault excitation of the rigid guides aggravates the horizontal vibration of the hoisting container. Although few magnetorheological dampers have been used in mine hoisting systems, some studies have used magnetorheological dampers in hoisting systems [28]. Therefore, this study investigated and designed a skyhook damping control strategy to suppress the horizontal vibration of the hoisting container. Magnetorheological dampers were used as cushioning devices to suppress horizontal vibrations in container. The horizontal vibration acceleration of the hoisting container was used as the evaluation indicator for vibration suppression. Therefore the control purpose in this study is to reduce the horizontal vibration acceleration at the centre of mass of the hoisting container.

Considering that the mine hoisting system is a multi-input and multi-output (MIMO) system, the state space equation was used in this paper to describe the equations of the model. From equation (9) the state vector $\mathbf{X}$, the control vector $\mathbf{U}$ and the disturbance vector $\mathbf{W}$ were expressed as

$$\mathbf{X} = \begin{bmatrix} \mathbf{q} \\ \mathbf{s} \\ \dot{\mathbf{q}} \\ \dot{\mathbf{s}} \end{bmatrix} \quad \mathbf{U} = \begin{bmatrix} f_{1x} \\ f_{2x} \\ f_{3x} \\ f_{4x} \end{bmatrix} \quad \mathbf{W} = \begin{bmatrix} \mathbf{r} \\ \dot{\mathbf{r}} \end{bmatrix}$$

From equation (10), the state-space equation of the mine hoisting system was expressed as

$$\dot{\mathbf{X}} = \mathbf{AX} + \mathbf{BU} + \mathbf{RW}$$

In this paper, the semi-active control strategy for horizontal vibration of mine hoisting systems was skyhook damping control. The idea of skyhook damping control is to install a skyhook damper between the control target and an imaginary

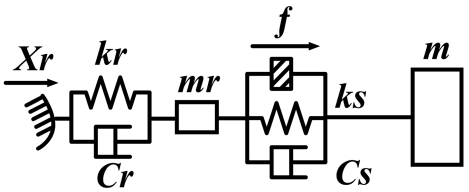

FIGURE 11. Horizontal vibration model for 1/4 mine hoisting system.

skyhook. The imaginary skyhook damper would only consume the energy of the control target. When the damping of the skyhook damper is adjusted to a suitable value, the vibration of the hoisting container will be effectively suppressed [29]. The dynamic model of the mine hoisting system was shown in Fig.2. To reduce the control difficulty, this study used the 1/4 horizontal vibration control model of the mine hoisting system, which is shown in Fig.11.

Equations for the 1/4 horizontal vibration control model were expressed as

$$\begin{aligned} m_r\ddot{x}_1 &= k_r\left(x_r - x_1\right) + c_r\left(\dot{x}_r - \dot{x}_1\right) \\ &\quad + k_s\left(x_0 - x_1\right) + c_s\left(\dot{x}_0 - \dot{x}_1\right) - f \\ m\ddot{x}_0 &= k_s\left(x_1 - x_0\right) + c_s\left(\dot{x}_1 - \dot{x}_0\right) + f \end{aligned}$$

where x_r is the displacement excitation of the rigid guide to the roller cage shoe, x_1 is the horizontal displacement of the roller cage shoe, x_0 is the horizontal displacement of the hoisting container support, m_r is the equivalent mass of the roller cage shoe, m_0 is the equivalent mass of the hoisting container support, k_r is the contact stiffness of the roller cage shoe, c_r is the contact damping of the roller cage shoe, k_s is the buffer stiffness of the roller cage shoe, c_s is the buffer damping of the roller cage shoe, and f is the controlled damping force of the magnetorheological damper.

As magnetorheological dampers are semi-active actuators [30], the damping force of the magnetorheological dampers does not always meet the force required by the skyhook damping controller. The skyhook damping control therefore was converted to semi-active control by measuring the vibrations of the hoisting container and the roller cage shoes. [31] The damping force of the magnetorheological damper is related to its coil current. Therefore, the damping force of the magnetorheological damper reaches a maximum value when the current reaches a maximum value of 1 A, and the damping force of the magnetorheological damper reaches a minimum value when the current reaches a minimum value of 0 A.

Thus, the equations of converting the skyhook damping control to semi-active control were expressed as

$$F = \begin{cases} f_{\max}\left(I = I_{max}, x, \dot{x}\right), & \dot{x}_0\left(\dot{x}_0 - \dot{x}_1\right) > 0 \\ f_{\min}\left(I = I_{min}, x, \dot{x}\right), & \dot{x}_0\left(\dot{x}_0 - \dot{x}_1\right) \le 0 \end{cases}$$

where x and $\dot{x}$ are the piston displacement and velocity respectively, f_{max} is the magnetorheological damper output force when the coil current is taken to a maximum value of 1 A, and f_{min} is the magnetorheological damper output force when the coil current is taken to a minimum value of 0 A.

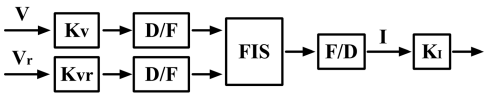

FIGURE 12. The working principle of fuzzy control.

The switching of the coil current between minimum and maximum values makes the magnetorheological damper and the mine hoisting system chatter [32]. Chattering not only shortens the life of magnetorheological dampers but also influences the stable operation of the system. In this study, several additional current options between the maximum and minimum currents of the magnetorheological damper were provided. More current options enabled magnetorheological dampers to switch output forces more smoothly. This control strategy can effectively suppress the vibrations of the hoisting container and contributes to the stability of the system.

By combining fuzzy control and skyhook damping control, a fuzzy skyhook damping controller has been designed. The controller divided the magnetorheological damper's coil current into seven options. Firstly, the fuzzy controller fuzzified the input signal into a fuzzy variable. Secondly, the fuzzy variable was transmitted to the fuzzy inference machine containing the fuzzy rules. Then the fuzzy inference machine obtained the fuzzy results by fuzzy operation. And finally, the fuzzy results were defuzzified into a current signal that can be used by the actuator. In the above process, fuzzification and defuzzification were completed through the fuzzification interface and defuzzification interface respectively. The main factor determining the effectiveness of fuzzy control is the fuzzy inference machine containing the fuzzy rules. [33] The working principle of fuzzy control was shown in Fig.12.

The fuzzy control system used a Mamdani type inference engine. The horizontal vibration speed V of the hoisting container and the relative vibration speed V_r between the hoisting container and roller cage shoe were used as inputs to the controller. And the magnetorheological damper coil current I was used as the output to the controller. Both the absolute velocity V and the relative velocity V_r were divided into nine fuzzy subsets. Triangle membership function was used as the membership function in this fuzzy controller. The fuzzy subsets of both absolute and relative velocities were denoted as {NB,NM,NS,NVS,ZE,PVS,PS,PM,PB}. And the fuzzy subsets stand for negative big, negative medium, negative small, negative very small, zero, positive very small, positive small, positive medium and positive big respectively. The universe of discourse for the absolute velocity V was taken as $\{-0.1,-0.075,-0.05,-0.025,0,0.025,0.05,0.075,0.1\}$. And the the universe of discourse for the relative velocity V_r was taken as $\{-0.2,-0.15,-0.1,-0.05,0,0.05,0.1,0.15,0.2\}$. The coil current I was divided into seven fuzzy subsets and the membership function used the triangle

TABLE 4. Fuzzy rule table for fuzzy skyhook damping control.

	V								
Vr	NB	NM	NS	NVS	ZE	PVS	PS	PM	PB
NB	PD	PC	PB	PA	PA	PA	PA	PA	PA
NM	PE	PD	PC	PB	PA	PA	PA	PA	PA
NS	PF	PE	PD	PC	PA	PA	PA	PA	PA
NVS	PG	PF	PE	PD	PA	PA	PA	PA	PA
ZE	PG	PG	PG	PG	PA	PG	PG	PG	PG
PVS	PA	PA	PA	PA	PA	PD	PE	PF	PG
PS	PA	PA	PA	PA	PA	PC	PD	PE	PF
PM	PA	PA	PA	PA	PA	PB	PC	PD	PE
PB	PA	PA	PA	PA	PA	PA	PB	PC	PD

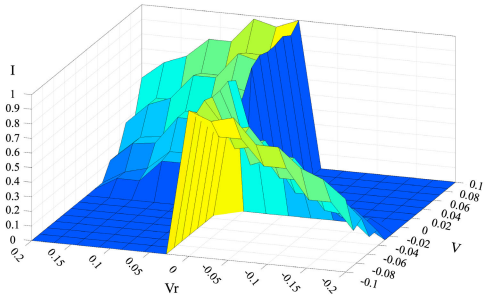

FIGURE 13. The 3D surfaces of the fuzzy rules.

membership function. The fuzzy subsets were denoted as {PA,PB,PC,PD,PE,PF,PG}. And the universe of discourse for the coil current I was taken as {0,0.15,0.3,0.55,0.7,0.85,1}. Thus, the magnetorheological damper had seven levels of coil current in total.

As both inputs were set to 9 fuzzy subsets, 81 fuzzy rules were generated in total. Magnetorheological dampers will chatter when the coil current is switched directly between minimum and maximum values. The control strategy that combines skyhook damping control with fuzzy control was effective in suppressing chatter generated by magnetorheological dampers [34]. The fuzzy rules for fuzzy skyhook damping control in this paper were shown in Table 4, and the three-dimensional surfaces of the fuzzy rules were shown in Fig.13.

Centroid of Area Method(centroid) was used to fuzzify fuzzy variables. [35] In order to match the fuzzification interface to the input signal, the input scaling gain was set before the fuzzification interface. And in order to match the defuzzification interface to the actuator, the output scaling gain was set after the defuzzification interface.

In order to compare with conventional control strategies, a PID semi-active controller was also designed in this study. The proportional-integral-derivative(PID) controller consists of the error, the integral of error and the derivative of error. The algorithm of the PID controller is simple and the stability of the controller is excellent. The PID controller can control the system effectively without an accurate system model.

The PID control algorithm can be expressed as:

$$u(t) = K_p e(t) + \frac{1}{K_i}\int e(t)\mathrm{d}t + K_d \frac{\mathrm{d}e(t)}{\mathrm{d}t}$$

where $e(t)$ is error of the system, K_p is the proportion coefficient, K_i is the integration coefficient, and K_d is the differentiation coefficient.

The controller weighted the error, the integral of error and the derivative of error respectively. The controller then fed the calculated control signal to the actuator of the control system. The horizontal vibration acceleration of the hoisting container was used as the control object for PID control. The deviation of the horizontal vibration acceleration from zero acceleration was used as the deviation signal for PID control. The trial and error method was used to adjust the PID parameters. And the final parameters were determined to be 4200 for K_p, 1/28200 for K_i and 50 for K_d.

Magnetorheological dampers are semi-active actuators, so it is necessary to convert the PID active control to semi-active control. In order to convert to semi-active control, the inverse model of magnetorheological damping needs to be solved. The desired control force of the Pid controller was converted into a semi-active output force of the magnetorheological damper. Firstly, the mathematical model of the magnetorheological damper was derived in reverse to obtain the inverse mathematical model of the magnetorheological damper. Secondly, the correctness of the inverse mathematical model was verified by simulation. Thirdly, the PID controller was constructed in the mine hoisting system. Then, the desired control force of the Pid controller was fed into the inverse mathematical model of the magnetorheological damper. Finally, the inverse mathematical model calculated the control current of the magnetorheological damper.

According to equation (11) and Table 3, the expression for the mathematical model of magnetorheological damping was as follows:

$$\begin{aligned}
&0 \leqslant I \leqslant 0.2:\\
&f = (579.6\,I + 82.96)\tanh(0.1\dot{x} + 0.065\,x)\\
&\quad + (3.1\,I + 0.71)\dot{x} + 0.27\,x - 19.95\,I - 11.77\\
&0.2 < I \leqslant 1:\\
&f = (-719.6\,I^2 + 1817I - 135.7)\tanh(0.075\dot{x} + 0.08\,x)\\
&\quad + (0.1429\,I^2 + 2.669\,I + 0.84)\dot{x} + 0.27\,x\\
&\quad + 16.28\,I^2 - 29.55\,I - 11.67
\end{aligned}$$

The above equations were derived backwards. The equations for the inverse mathematical model of magnetorheological damping were expressed as

$$\begin{aligned}
&0 \leqslant I \leqslant 0.2:\\
&I = \frac{f_1 - 82.96\tanh(0.1\dot{x}+0.065\,x) - 0.71\dot{x} - 0.27\,x + 11.77}{579.6\tanh(0.1\dot{x} + 0.065\,x) + 3.1\dot{x} - 19.95}\\
&0.2 < I \leqslant 1:\\
&0 = [-719.6\tanh(0.075\dot{x} + 0.08\,x) + 0.1429\dot{x} + 16.28]I^2\\
&\quad + [1817\tanh(0.075\dot{x} + 0.08\,x) + 2.669\dot{x} - 29.55]I
\end{aligned}$$

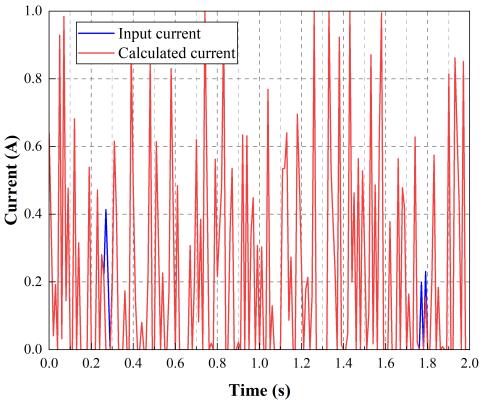

FIGURE 14. The simulation results for the current signal.

$$-135.7\tanh(0.075\dot{x}+0.08\,x)+0.84\dot{x}$$
$$+0.27\,x-11.67-f_2$$

Based on the above equations, the inverse model of magnetorheological damper was built in Simulink. Before using the inverse model of magnetorheological dampers, the validity of the inverse model needs to be verified. A Sine signal with an amplitude of 2 cm and a vibration frequency of 1 HZ was used as the vibration excitation. A normally distributed random number with a variance of 0.3 and a mean of 0 was used as the current signal for the magnetorheological damper model. Finally, the input current signal was compared with the current signal calculated by the inverse model to verify the validity of the inverse model. The simulation results for the current signal are shown in Fig.14.

As shown in Fig.14, the results for both current signals were essentially the same. Both models obtained the same current signal with the same excitation signal, which verified the correctness of the inverse model.

B. ADAMS/SIMULINK CO-SIMULATION

In this study Adams/Simulink co-simulation was used to test horizontal vibration control algorithms for mine hoisting systems. In the simulation process, the vibration signal of the mine hoisting system in Adams was output to Simulink in real time. Then, the controller designed in Simulink was used to operate on this signal. Finally, the operation results from Simulink were sent back to the mine hoisting system in Adams. In Adams, the vibration signals of the hoisting container, the roll cage shoe and the fixed support were set as output variables respectively. And the damping forces of the magnetorheological dampers were set as input variables. Then, the input and output variables were connected to the Matlab platform via the Adams Controls Plant Export module. The co-simulation control process of fuzzy skyhook control and PID semi-active control were shown in in Fig.15. and Fig.16 respectively.

After entering the "Adams_sys" command in the Matlab platform, the Adams Subsystem module was called

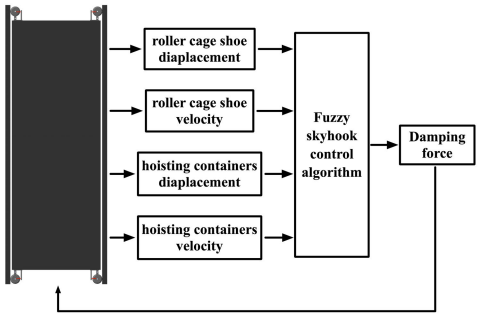

FIGURE 15. The control process of fuzzy skyhook control.

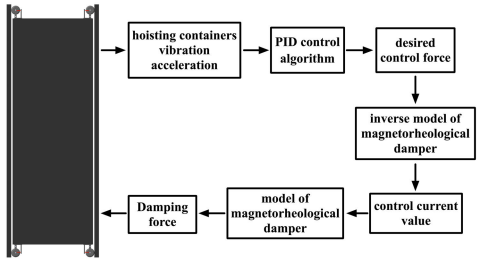

FIGURE 16. The control process of PID semi-active control.

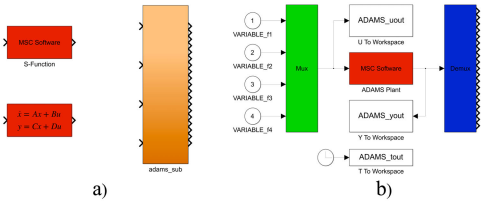

FIGURE 17. (a) Adams Subsystem module. (b) Adams Plan module.

and displayed in Simulink. The Adams Subsystem module contains the Adams Plant block, which can modify the co-simulation parameters. In the Adams Plant block, the simulation step size was set to 0.001 s and the co-simulation mode was set to real-time interactive mode. The Adams Subsystem module and Adams Plan block are shown in Fig.17.

The fuzzy skyhook damping controller and the PID semi-active controller were designed in Simulink. The fuzzy skyhook damping controller, PID semi-active controller, magnetorheological damper model and Adams Subsystem module were connected together. Firstly, the operating results of the Adams model of the mine hoisting system were transmitted to the fuzzy skyhook damping controller and the PID semi-active controller respectively. Secondly, the control currents of the magnetorheological dampers were calculated separately by the two controllers. Then, after combined with the magnetorheological damper model, these two controllers calculated the output force of the magnetorheological damper separately. Finally, the output forces calculated by both control strategies were transmitted back to the mine hoisting system model in Adams via the Adams Subsystem module.

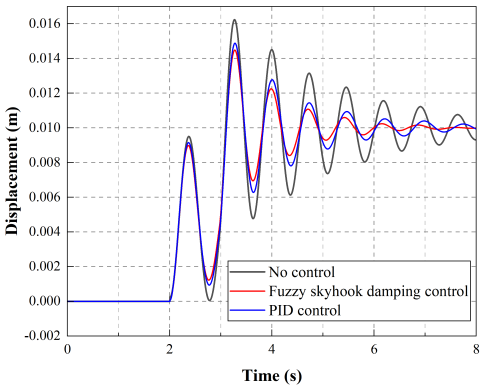

FIGURE 18. Displacement response for the hoisting container.

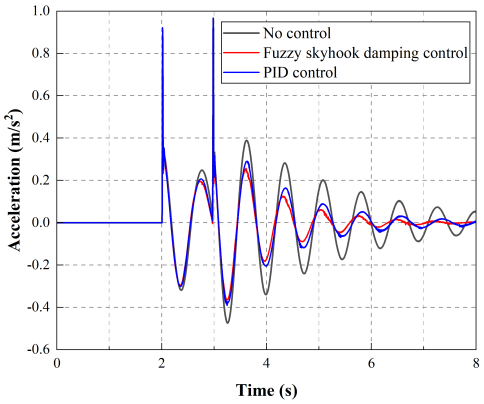

FIGURE 19. Acceleration response for the hoisting container.

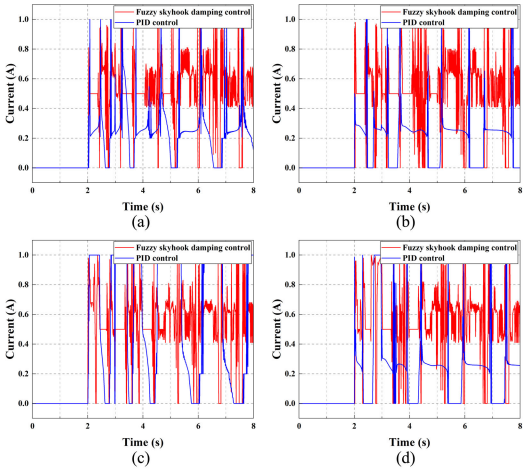

FIGURE 20. The current signals of magnetorheological dampers: (a) Damper for the upper roller cage shoe on the side of the faulty rail, (b) Damper for the upper roller cage shoe on the side of the intact rail, (c) Damper for the lower roller cage shoe on the side of the faulty rail, and (d) Damper for the lower roller cage shoe on the side of the intact rail.

TABLE 5. The control results for different control strategies.

Controller	RMS	Mean value	Maximum value
No Control	0.1682	-0.0120	0.3894
Fuzzy skyhook damping control	0.0886 (↓ 47.32%)	0.0093 (↓ 22.50%)	0.2516 (↓ 35.39%)
PID semi-active control	0.1106 (↓ 34.24%)	-0.0106 (↓ 11.67%)	0.2911 (↓ 25.24%)

C. ANALYSIS OF VIBRATION CONTROL RESULTS

The hoisting speed was set to 9 m/s and the step height of the rigid guide was set to 2 cm in Adams. The running time was set to 8 s in Simulink. The horizontal vibration acceleration and displacement of the hoisting container were used as evaluation indicators. Finally, Adams/Simulink co-simulation of the mine hoisting system was carried out. The simulation results for the horizontal vibration of the mine hoisting container were shown in Figs.18 and 19. And the current signals of the four magnetorheological dampers were shown in Figs.20.

From the response of the acceleration and displacement, both control strategies can effectively suppress the horizontal vibration of the mine hoisting container caused by the guide misalignment failures. In order to compare the control effects from different controllers, the simulation results need to be expressed quantitatively. The root mean square(RMS), mean and maximum values for the horizontal vibration acceleration were calculated after all roller cage shoes had passed through the misaligned rigid guides.

Root Mean Square Error(RMSE) is the standard deviation of the residuals. RMSE is usually used to measure the dispersion of these residuals. The mean value for the acceleration was the sum of all sampled accelerations divided by the number of samples. And the maximum value of the acceleration was the largest of all sampled accelerations. The RMS, mean and maximum values for the horizontal vibration acceleration can be expressed as:

$$A_{\mathrm{RMS}} = \left[\sum_{i=1}^{N} (a_i - a_0)^2 / N\right]^{\frac{1}{2}}$$

$$\bar{A} = \frac{1}{N}\left(\sum_{i=1}^{N} a_i\right)$$

$$A_{\max} = \mathrm{Max}\{a_1, a_2 \cdots, a_N\}$$

where a_i is the sampled horizontal vibration acceleration after all roller cage shoes had passed through the misaligned rigid guides, a_0 is the 0 acceleration value, and N is the number of sampled horizontal vibration acceleration after all roller cage shoes had passed through the misaligned rigid guides. The control results for different control strategies were shown in Table 5.

With the use of fuzzy skyhook damping control, the RMS value of horizontal vibration acceleration was reduced by 47.32%, the mean value by 22.50% and the maximum value by 35.39%. Further, with the use of PID semi-active control, the RMS value of horizontal vibration acceleration was reduced by 34.24%, the mean value by 11.67% and the maximum value by 25.24%. According to the simulation

results, it can be seen that both control strategies have good suppression effect on the horizontal vibration of the mine hoisting system. By observing the evaluation indicators of acceleration, it can be seen that the fuzzy skyhook damping controller suppresses the horizontal vibration of the hoisting container better than the PID semi-active controller. The reason for this result may be that conventional PID control cannot adjust the control parameters in real time as the system operates. And, the semi-active damping force of the magnetorheological dampers does not always meet the active control force expected from the PID controller. As a result, the fuzzy skyhook damping control showed better effect on vibration suppression.

VI. CONCLUSION

In this paper, the magnetorheological dampers were innovatively introduced into the mine hoisting system by adding the semi-active vibration damping cushion on the roller cage shoe. And the feasibility of the magnetorheological damper for suppressing horizontal vibration of the mine hoisting container was demonstrated.

This study modelled the mine hoisting system. A mathematical model and a virtual prototype model for the 2-degree-of-freedom horizontal vibration of the mine hoisting system were established, which provides the model basis for the horizontal vibration control of the mine hoisting system.

Compared to floating sheaves, the roller cage shoes as actuators have no time lag effect when the actuators control the vibration of the system. And there is no excess unknown disturbance between the actuator and the mine hoisting container. The use of magnetorheological dampers in roller cage shoes is a cost-effective and less difficult method to suppress vibrations.

The RMS, mean and maximum values for the horizontal vibration acceleration of the hoisting container were reduced by 47.32%, 22.50% and 35.39% respectively, which was a relatively significant effect for vibration control. The simulation results showed that the fuzzy skyhook control strategy not only successfully suppresses the horizontal vibration of the mine hoisting container, but also has better effect than the traditional PID control. This study provided an effective reference for the horizontal vibration control strategy of the mine hoisting system. If both floating sheaves and roller cage shoes are used as control actuators, the vibration of the mine hoisting container will be further suppressed.

REFERENCES

[1] M. M. Khan and G. J. Krige, "Evaluation of the structural integrity of aging mine shafts," *Eng. Struct.*, vol. 24, no. 7, pp. 901–907, Jul. 2002.

[2] J. Jakubowski and P. Fiołek, "Evaluation of stiffness and dynamic properties of a mine shaft steelwork structure through in situ tests and numerical simulations," *Energies*, vol. 14, no. 3, p. 664, Jan. 2021.

[3] M. Plachno, "Mathematical model of transverse vibrations of a high-capacity mining skip due misalignment of the guiding tracks in the hoisting shaft," *Arch. Mining Sci.*, vol. 63, no. 1, pp. 3–26, 2018.

[4] S. Kaczmarczyk and W. Ostachowicz, "Transient vibration phenomena in deep mine hoisting cables. Part 1: Mathematical model," *J. Sound Vibrat.*, vol. 262, no. 2, pp. 219–244, Apr. 2003.

[5] D. Wang, D. Zhang, and S. Ge, "Effect of terminal mass on fretting and fatigue parameters of a hoisting rope during a lifting cycle in coal mine," *Eng. Failure Anal.*, vol. 36, pp. 407–422, Jan. 2014.

[6] Y. Wang, G. Cao, and W. T. van Horssen, "Dynamic simulation of a multi-cable driven parallel suspension platform with slack cables," *Mechanism Mach. Theory*, vol. 126, pp. 329–343, Aug. 2018.

[7] Y. Wang, G. Cao, and Z. Zhu, "Longitudinal response of parallel hoisting system with time-varying rope length," *J. Vibroengineering*, vol. 16, no. 8, pp. 4088–4101, 2014.

[8] Y. Guo, D. Zhang, X. Zhang, S. Wang, and W. Ma, "Experimental study on the nonlinear dynamic characteristics of wire rope under periodic excitation in a friction hoist," *Shock Vibrat.*, vol. 2020, pp. 1–14, Feb. 2020.

[9] J. Wu and Z. Kou, "Theoretical coupling longitudinal-transverse model and experimental verification of transverse vibration of rope for multi-rope friction hoisting system," *Int. J. Coal Sci. Technol.*, vol. 3, no. 1, pp. 77–84, Mar. 2016.

[10] G. Cao, J. Wang, and Z. Zhu, "Coupled vibrations of rope-guided hoisting system with tension difference between two guiding ropes," *Proc. Inst. Mech. Eng., C, J. Mech. Eng. Sci.*, vol. 232, no. 2, pp. 231–244, Jan. 2018.

[11] D.-H. Yang, K.-Y. Kim, M. K. Kwak, and S. Lee, "Dynamic modeling and experiments on the coupled vibrations of building and elevator ropes," *J. Sound Vibrat.*, vol. 390, pp. 164–191, Mar. 2017.

[12] J. Wang, S.-X. Tang, Y. Pi, and M. Krstic, "Exponential regulation of the anti-collocatedly disturbed cage in a wave PDE-modeled ascending cable elevator," *Automatica*, vol. 95, pp. 122–136, Sep. 2018.

[13] X. Li, Z.-C. Zhu, and G. Shen, "A switching-type controller for wire rope tension coordination of electro-hydraulic-controlled double-rope winding hoisting systems," *Proc. Inst. Mech. Eng., I, J. Syst. Control Eng.*, vol. 230, no. 10, pp. 1126–1144, Nov. 2016.

[14] J. Yao, Y. Ma, C. Ma, X. Xiao, and T. Xu, "Effect of misalignment failures of steel guides on impact responses in friction mine hoisting systems," *Eng. Failure Anal.*, vol. 118, Dec. 2020, Art. no. 104841.

[15] Y. Li, J. Xue, X. Zhang, J. Song, and H. Jing, "Design of experimental platform for the static stiffness of guide roller," in *Proc. Int. Conf. Mech. Mater. Aerosp. Eng.*, May 2017, pp. 17–22.

[16] K.-Y. Chen, M.-S. Huang, and R.-F. Fung, "Dynamic modelling and input-energy comparison for the elevator system," *Appl. Math. Model.*, vol. 38, nos. 7–8, pp. 2037–2050, Apr. 2014.

[17] X. Li, Z. Zhu, D. Cheng, G. Shen, and Y. Tang, "A robust nonlinear controller with low-gain-state-observer for wire rope tension active control of hoisting systems," *IEEE Access*, vol. 8, pp. 111208–111222, 2020.

[18] Z.-C. Zhu, X. Li, G. Shen, and W.-D. Zhu, "Wire rope tension control of hoisting systems using a robust nonlinear adaptive backstepping control scheme," *ISA Trans.*, vol. 72, pp. 256–272, Jan. 2018.

[19] N. V. Gaiko and W. T. van Horssen, "Resonances and vibrations in an elevator cable system due to boundary sway," *J. Sound Vibrat.*, vol. 424, pp. 272–292, Jun. 2018.

[20] J. Wang, Y. Pi, Y. Hu, and Z. Zhu, "State-observer design of a PDE-modeled mining cable elevator with time-varying sensor delays," *IEEE Trans. Control Syst. Technol.*, vol. 28, no. 3, pp. 1149–1157, May 2020.

[21] X. Chen, Z. Zhu, G. Shen, and W. Li, "Tension coordination control of double-rope winding hoisting system using hybrid learning control scheme," *Proc. Inst. Mech. Eng., I, J. Syst. Control Eng.*, vol. 233, no. 10, pp. 1265–1281, Nov. 2019.

[22] J. Wang, Y. Pi, Y. Hu, and X. Gong, "Modeling and dynamic behavior analysis of a coupled multi-cable double drum winding hoister with flexible guides," *Mechanism Mach. Theory*, vol. 108, pp. 191–208, Feb. 2017.

[23] A. Muhammad, X.-L. Yao, and Z.-C. Deng, "Review of magnetorheological (MR) fluids and its applications in vibration control," *J. Mar. Sci. Appl.*, vol. 5, no. 3, pp. 17–29, Sep. 2006.

[24] A. G. Olabi and A. Grunwald, "Design and application of magneto-rheological fluid," *Mater. Design*, vol. 28, no. 10, pp. 2658–2664, Jan. 2007.

[25] A. Ashfak, A. Saheed, K. K. A. Rasheed, and J. A. Jaleel, "Design, fabrication and evaluation of mr damper," *Int. J. Aerosp. Mech. Eng.*, vol. 1, pp. 27–33, Mar. 2011.

[26] L. Balamurugan, J. Jancirani, and M. A. Eltantawie, "Generalized magnetorheological (MR) damper model and its application in semi-active control of vehicle suspension system," *Int. J. Automot. Technol.*, vol. 15, no. 3, pp. 419–427, Apr. 2014.

[27] S. Wei, J. Wang, and J. Ou, "Experimental study on inverse model-based force tracking control of MR damper," *Shock Vibrat.*, vol. 2020, pp. 1–14, Sep. 2020.

[28] R. Monge, J. M. Rodríguez-Fortún, A. Gómez, J. A. Roig, and P. González, "Design of semi-active roller guides for high speed elevators," *Appl. Mech. Mater.*, vol. 706, pp. 108–116, Dec. 2014.
[29] N. D. Sims and R. Stanway, "Semi-active vehicle suspension using smart fluid dampers: A modelling and control study," *Int. J. Vehicle Des.*, vol. 33, nos. 1–3, pp. 76–102, 2003.
[30] C.-W. Zhang, J.-P. Ou, and J.-Q. Zhang, "Parameter optimization and analysis of a vehicle suspension system controlled by magnetorheological fluid dampers," *Structural Control Health Monitor.*, vol. 13, no. 5, pp. 885–896, 2006.
[31] K. Hemanth, H. Kumar, and K. V. Gangadharan, "Vertical dynamic analysis of a quarter car suspension system with MR damper," *J. Brazilian Soc. Mech. Sci. Eng.*, vol. 39, no. 1, pp. 41–51, Jan. 2017.
[32] M. Ahmadian, X. Song, and S. C. Southward, "No-jerk skyhook control methods for semiactive suspensions," *J. Vibrat. Acoust.*, vol. 126, no. 4, pp. 580–584, Oct. 2004.
[33] J. Mendes, R. Maia, R. Araújo, and F. A. A. Souza, "Self-evolving fuzzy controller composed of univariate fuzzy control rules," *Appl. Sci.*, vol. 10, no. 17, p. 5836, Aug. 2020.
[34] T. Ma, F. Bi, X. Wang, C. Tian, J. Lin, J. Wang, and G. Pang, "Optimized fuzzy skyhook control for semi-active vehicle suspension with new inverse model of magnetorheological fluid damper," *Energies*, vol. 14, no. 6, p. 1674, Mar. 2021.
[35] N. K. Arun and B. M. Mohan, "Modeling, stability analysis, and computational aspects of some simplest nonlinear fuzzy two-term controllers derived via center of area/gravity defuzzification," *ISA Trans.*, vol. 70, pp. 16–29, Sep. 2017.

XIAOJIE DENG was born in Sanming, Fujian, China, in 1999. He received the B.S. degree in mechanical engineering from the China University of Mining and Technology, Beijing, in 2021. He is currently pursuing the M.S. degree in mechanical engineering with the School of Mechanical Engineering, Nantong University.

JIANNAN YAO received the Ph.D. degree in mechatronic engineering from the China University of Mining and Technology, Xuzhou, China, in 2016. He is currently an Associate Professor with the School of Mechanical Engineering, Nantong University, China. His current research interests include mechanical dynamics and mechatronics.

DI LIU was born in Fuyang, Anhui, China, in 1999. He received the B.S. degree in mechanical engineering from Nantong University, Nantong, China, in 2020, where he is currently pursuing the M.S. degree in mechanical engineering with the School of Mechanical Engineering.

RUI YAN was born in Datong, Shanxi, China, in 1996. She received the B.S. degree in mechanical engineering from the Beijing University of Posts and Telecommunications, Beijing, China, in 2019. She is currently pursuing the M.S. degree in mechanical engineering with the School of Mechanical Engineering, Nantong University.